Nadir Margins in TerraSAR-X Timing Commanding

S. Wollstadt and J. Mittermayer, *Member, IEEE*

***Abstract*—This paper presents an analysis and discussion of the Nadir return in the context of radar timing. Results obtained during the Commissioning Phase of TerraSAR-X in verification and measurement of Nadir return and timing margins are shown. Pre-launch assumptions about the Nadir margins were verified and optimized, which led to an improvement in the timing commanding, i.e. a relaxing of the timing. By means of three early acquired TerraSAR-X images which contain Nadir returns their characteristic properties are shown and explained.**

***Index Terms*—Nadir, radar timing, TerraSAR-X**

I. Introduction

TerraSAR-X is the first German Radar Satellite for scientific and commercial applications. It is a high resolution Synthetic Aperture Radar at X-Band and was launched on June, 15th 2007. In the Commissioning Phase the overall SAR performance was characterized and verified. The analysis and verification of the margins in the radar timing (fast time) commanding was part of the overall SAR performance analysis. In this paper the Nadir timing, especially the margin analysis, is presented and discussed. The Nadir point is defined as the point on-ground with the closest distance to the satellite. At small incidence angles – incidence angle at Nadir point is around 0° – the signal is directly reflected to the sensor and a single slant range resolution cell covers a large area on-ground. Therefore the backscattered reflections of the transmitted signal from the Nadir area (around the Nadir point) can be stronger than in far range and may appear as a bright ambiguity in the processed SAR image. In order to overcome this problem the Nadir return must be considered in the timing calculation. Since the timing in TerraSAR-X is very narrow due to the relatively high pulse repetition frequency (PRF) and due to the relatively large desired scene size the Nadir return duration is to be estimated very accurately. This paper presents the investigations made during the commissioning phase in order to measure and verify timing margins w.r.t. the Nadir return.

The paper is structured as follows. The determination of the Nadir angle and the verification that the receiver will not be in saturation, are explained in section II together with the corresponding timing description. Section III shows some erroneous acquired results of the early Commissioning Phase, i.e. some Nadir images, along with the corresponding explanation of the acquired Nadir returns and its characteristics. In section IV the analysis of the Nadir assumptions is presented. Section V presents the extension of the existing Nadir margins due to errors in the Digital Elevation Model which resolved the problem of a few images with Nadir returns. Finally section VI concludes the paper with a discussion about the lessons-learned and the improvement of the timing strategy.

S. Wollstadt and J. Mittermayer are with the German Aerospace Center, 82234 Oberpfaffenhofen, Germany. (phone: +49-8153-282376; e-mail: steffen.wollstadt@dlr.de).

II. Margin Assumptions

A. TerraSAR-X Timing

The pre-launch TerraSAR-X timing calculation was driven by two major constraints. First, the required pulse repetition frequency is relatively high with approximately 3000 to 6500 Hz and second, the swath width is supposed to be kept constant at 30 km for single and 15 km for dual polarizations, respectively. Since the Spotlight mode scene extension is 10 km, no problems were expected to arise in this mode. Furthermore no changes in the pulse repetition frequency are allowed in a basic product datatake length of 50 km, i.e. approximately 8 seconds of acquisition time. This means, that the pulse repetition interval also has to consider a possible sliding of the echo window across the acquired scene. In order to ensure the integrity of the scene, margins for the receiving window were introduced for errors in orbit prediction, range cell migration, pointing and the Digital Elevation Model used in the command generation.

B. Nadir Timing Margins

The Nadir return is a range ambiguous echo of a transmitted pulse which is to be considered in the timing calculation, since it might be very strong due to the geometrical situation, i.e. specular reflections. Therefore the Nadir return duration has to be calculated and considered in the choice of the pulse repetition frequency. Fig. 1 shows a timing plot and illustrates a timing situation with a certain pulse repetition frequency at the instance of fast time when the first echo window reaches the receiving antenna. As it can be seen, the Nadir return is a limiting factor in the PRF selection since it reduces the available time for the receiving echo window within the PRI. In order to mitigate its influence, it is important to determine the duration of the Nadir pulse as precise as possible.

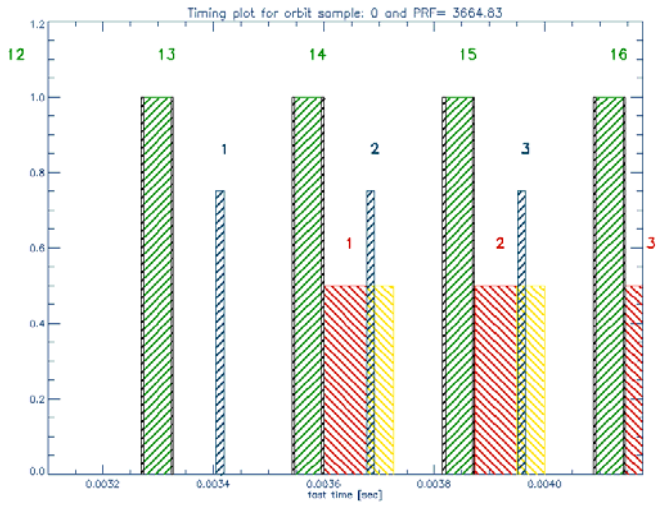

Fig. 1. Timing plot with TX event (green), Nadir event (blue) and receiving window (focused echo window (red) and extension by pulse length (yellow))

Before the TerraSAR-X launch two major assumptions were made in the timing calculation concerning the Nadir return. First, the Nadir (elevation) angle corresponding to the Nadir reflection area on-ground was assumed conservatively to be +/- 5°. This nadir angle corresponds to approximately 13 µs Nadir pulse duration.

The second assumption was that the receiver will not be in saturation when a Nadir return is received. If the energy of the Nadir return would cause a saturation of the receiver, the affected "image area" of the focused echo window could not be focused correctly. It is necessary, that Nadir and signal energy can be separated within the compression step of processing. This is a precondition for allowing the Nadir return in the pulse length right after the focused echo window but still in the overall receiving window. The pulse length after the focused echo window is necessary to compress each point of the focused echo window with the whole bandwidth of the chirp, but only the valid focused echo window is selected after SAR processing. Allowing the Nadir at the end of the echo window means therefore a benefit of one pulse length in the timing calculation, e.g. approximately 50 µs are additionally useable for a typical PRF of TerraSAR-X.

III. CP Nadir Characterization

A. Nadir return in TerraSAR-X images

During the Commissioning Phase (CP) of TerraSAR-X in 14 of 4300 operator-checked images Nadir returns were detected. Almost all of them were located in near range beam acquisitions where the antenna sidelobes are adjacent to the main lobe and thus generally higher than in far range. Fig. 2 to Fig. 4 show three of the few Nadir images with different intensities of the Nadir return. All images are taken at near range beam strip_003.

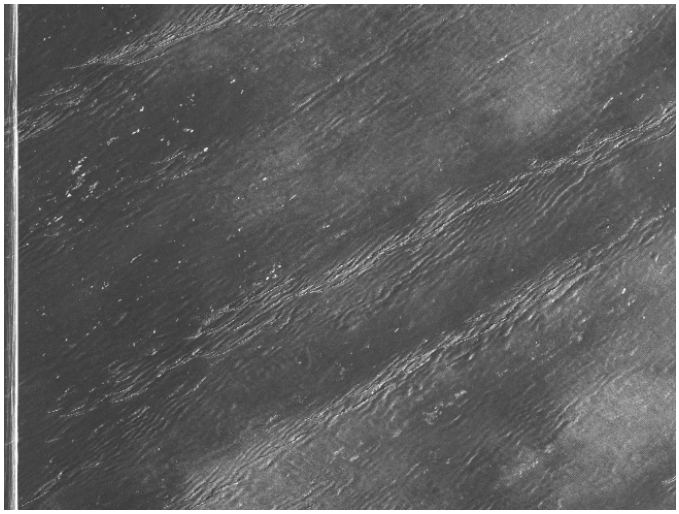

Fig. 2. Datatake with strong Nadir return at left side (far range) of image: Mali, Africa [lat:19.08°, lon:-3.45°]. (descending orbit, right-looking, top of image~North)

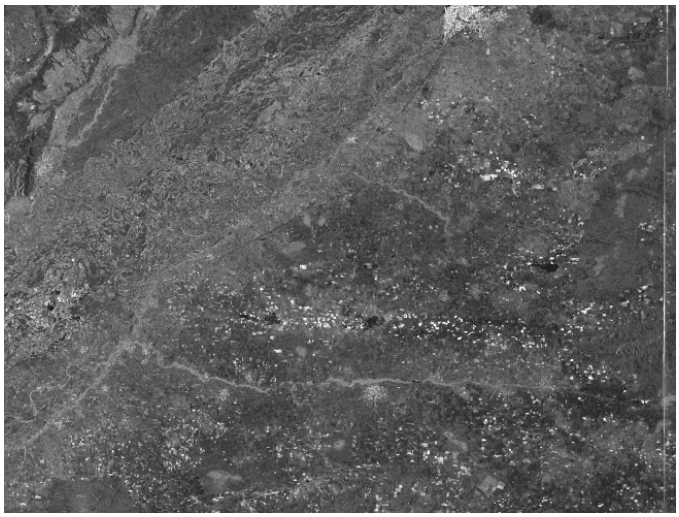

Fig. 3. Datatake with Nadir return with alternating intensity at right side (far range) of image: Nigeria, Africa [lat:12.62°, lon:-4.48°]. (ascending orbit, right-looking, top of image~North)

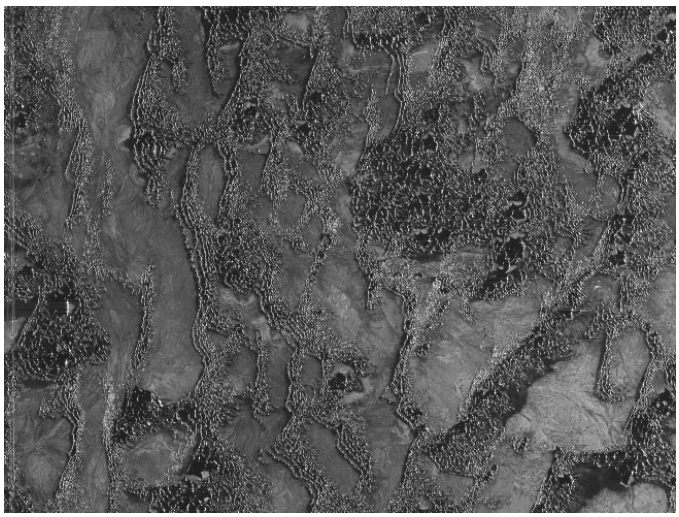

Fig. 4. Datatake with weak Nadir return at left side (far range) of image: Algeria, Africa [lat:28.38°, lon:-3.68°]. (descending orbit, right-looking, top of image~North)

As it can be seen, all Nadir returns appear in the far range of each image, which was the same for the other detected Nadir images. The explanation for this occurrence is the before mentioned pre-launch Nadir angle assumed to be +/-5°. These theoretical angles (0° at approximately Nadir point to +/-5°) practically correspond to exactly the time where the Nadir point echo returns and the maximum time from where the last Nadir echo is received. This means, since the Nadir angle was chosen large, the Nadir timing has a large margin in its falling edge. I.e. if the Nadir return is before the receiving window, there is a margin before the near range of the image. But if the Nadir return is directly after the focused echo window (refer to Fig. 1), there is no margin in Nadir timing in its rising edge and a Nadir return may appear in the image far range. These facts are illustrated in Fig. 5. The aspect of the Nadir return being inside the SAR image will be covered in section V in more detail.

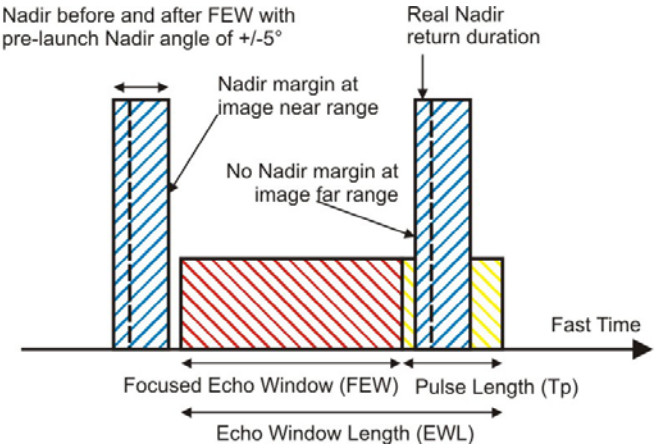

Fig. 5. Illustration of pre-launch Nadir timing margins in fast time. FEW is focused echo window.

B. *Nadir return characteristics*

Nadir returns in SAR images have mainly three characteristics: the intensity, the width and the course, i.e. the range position along azimuth. A closer look to Fig. 3 reveals that the Nadir return runs slightly diagonal or is shifted a little bit from left to right. This is caused by the height profile on-ground, i.e. the distance between satellite and the Nadir point varies along azimuth. In Fig. 3 the satellite height has to have an increasing slope with azimuth since the Nadir return is received slightly later at the end of the acquisition (top of the figure). In Fig. 6 the satellite height of the Nadir area of this image along azimuth is shown as measured by the Nadir analysis. As can be seen, the distance increases by around 130 m which is approximately 0.9 µs in timing. The satellite height was evaluated by calculating the fast time when the Nadir return appears in each range compressed rangeline (cp. section IV.B).

The intensity and the width (cp. Fig. 3) of the Nadir return in a SAR image are related to each other. Their modulation result from the backscatter value on-ground as well as from the signal-to-Nadir-ratio. In case the backscatter of the Nadir area increases or the signal intensity, i.e. backscatter of the acquisition area, decreases, the overall brightness of the Nadir return increases and therefore also its width can become broader. Fig. 3 leads also to the conclusion that there must be Nadir areas with very weak backscattering so that no Nadir return is visible although it is inside the receiving echo window.

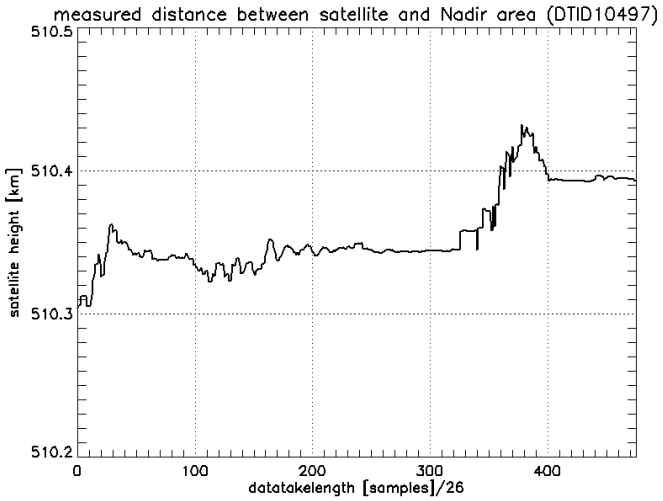

Fig. 6. Calculated satellite height over Nadir area along azimuth direction of datatake shown in Fig. 3.

IV. Analysis and Verification

A. *Commanded System-Datatakes*

In the raw data of an image containing a Nadir return, the energy of the signal and the Nadir return are received together in each rangeline or echo window, respectively. I.e. only the sum of both signals is available and they can not be analyzed separately. In order to analyze the pure Nadir return special system datatakes were generated and commanded. The system datatakes consists basically of the same radar instrument commands as for the images with the observed Nadir return (e.g. datatake Fig. 2). The only difference is that after each transmit pulse a sequence of "Receive Only" pulses was sent. This means, the instrument is during this PRI in receive mode, but not transmitting any pulses. The sequence was chosen to be longer than the number of traveling pulses of this datatake, i.e. typically around 13 for the near range swath strip_003. The number of traveling pulses of the Nadir return is then 12, i.e. the Nadir return of the same transmitted pulse arrives one PRI earlier than the desired SAR signal. This approach leads to a dataset, which contains in each sequence 1) one rangeline containing the desired SAR signal, 2) one rangeline with only the Nadir return and 3) many rangelines with noise only.

B. *Range-compressed Nadir return*

In order to derive the minimum necessary Nadir return duration in timing commanding as precise as possible, a

range-compression was performed on the raw data of the system datatakes depicted above. Then the rangeprofile was calculated from all rangelines containing only the received SAR signal as well as on the rangelines with only the Nadir returns. Fig. 7 to Fig. 9 show the two profiles of the datatakes shown in Fig. 2 to Fig. 4.

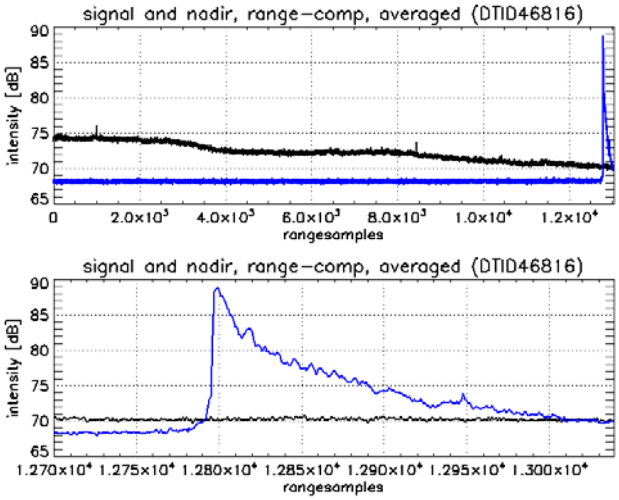

Fig. 7. Rangeprofile of range-compressed raw data of the system datatake corresponding to datatake in Fig. 2. Above: whole elevation range, Below: zoom to nadir area. (Black: Signal + noise, Blue: Nadir return + noise)

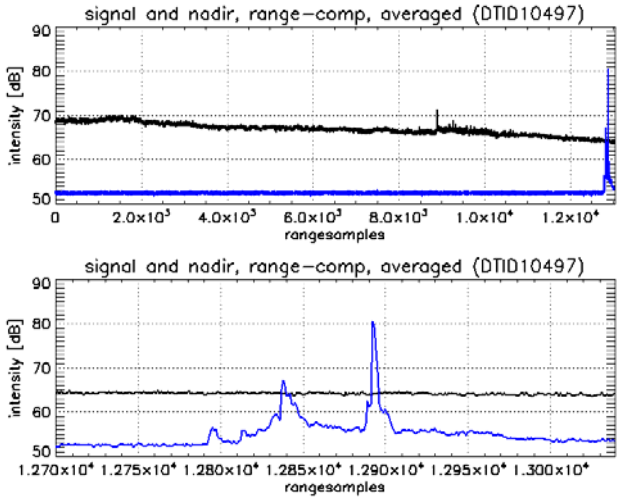

Fig. 8. Rangeprofile of range-compressed raw data of the system datatake corresponding to datatake in Fig. 3. Above: whole elevation range, Below: zoom to nadir area. (Black: Signal + noise, Blue: Nadir return + noise)

As is expected due to different signal and Nadir strength in all acquisitions all figures show different intensity levels for signal and Nadir. The signal level is different since it is strongly dependent on the backscatter of the acquired area. The noise level (in the near range of the Nadir range profile) is also different in each datatake. However, after applying the RX gain setting the noise level is the same for each datatake. The intensity and shape of the Nadir return pulse is also different in each datatake. The intensity is as a matter of course also dependent on the backscatter of the nadir area. Considering the shape of the figures above one has to keep in mind, that a complete rangeprofile is shown, i.e. the averaged sum over all rangelines. Due to the heightprofile of the Nadir area explained in section III.B the Nadir return changes its position within the acquired image. A nice shape of a Nadir return can be seen in Fig. 7. This is due to a flat Nadir area along the full datatake length.

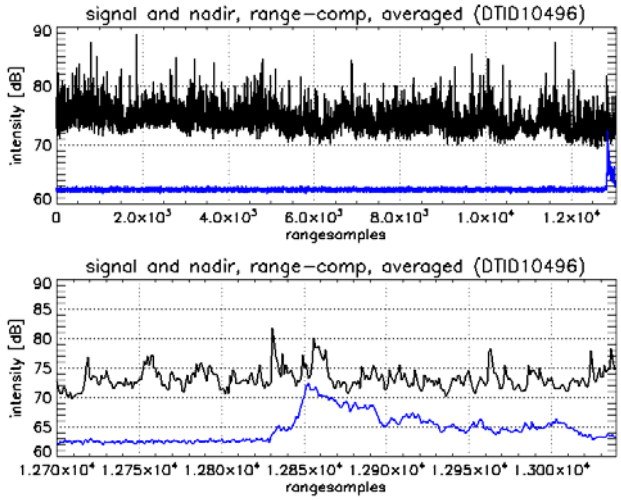

Fig. 9. Rangeprofile of range-compressed raw data of the system datatake corresponding to datatake in Fig. 4. Above: whole elevation range, Below: zoom to nadir area. (Black: Signal + noise, Blue: Nadir return + noise)

C. Estimation of Nadir pulse width

The datatake in Fig. 2 is a worst case w.r.t all detected datatakes in terms of visible Nadir returns which is a result of the very high signal-to-Nadir-ratio and the flat terrain (see Fig. 7). The scene has a low signal-to-noise-ratio since the acquired image shows desert area. The flat Nadir area results in an almost ideal Nadir return pulse shape in the range profile. Due to these conditions this datatake was selected as the reference for determining the Nadir angle width, i.e. the Nadir return duration in timing commanding. The whole pulse was taken into account. This means the whole width until the pulse vanishes into the noise level was considered. After measuring the number of samples of the Nadir pulse the pulse duration was estimated to be 1.2 µs, which corresponds to a maximum Nadir lookangle of 1.5°.

D. Saturation of Receiver / Nadir after focused echo window

The second assumption in section II.B, that the Nadir return is allowed in the pulselength extension after the focused echo window since the raw data are not saturated, was verified with a Nadir datatake where the nadir return is visible in the image, i.e. is *inside* the focused echo window. If the raw data of such a datatake is not in saturation, this holds also for a Nadir return which is outside the focused echo window. Fig. 10 shows that the raw data of a typical rangeline of the (imaging) worst case datatake in Fig. 2 is not in saturation, i.e. smaller than +/-128. The raw data contains the energy of signal and Nadir return.

In order to visualize the "impact" of the Nadir return in terms of raw data, Fig. 11 shows two rangelines of the system datatake derived from the strong Nadir datatake in Fig. 2 which contains rangelines with a Nadir return without SAR signal. The upper plot in Fig. 11 shows the preceding rangeline containing only noise, the lower plot shows noise and the Nadir return. The energy of the uncompressed Nadir return is strongly smeared over fast time but still visible in the far range of the range samples by slightly increasing amplitudes. In the raw data it is hardly to see, but in the SAR image and the range compressed data the Nadir return is strongly present. This slight increase of the raw data amplitudes has no major impact on the total signal amplitude strength and is therefore negligible in terms of saturation. Note the different scaling of the y-axis in Fig. 10 and Fig. 11.

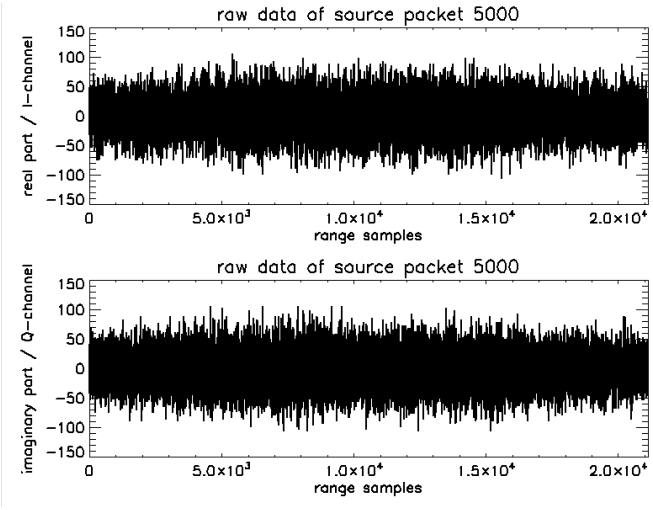

Fig. 10. Typical raw data rangeline of Nadir datatake in Fig. 2: Signal and Nadir return. (I- and Q-channel)

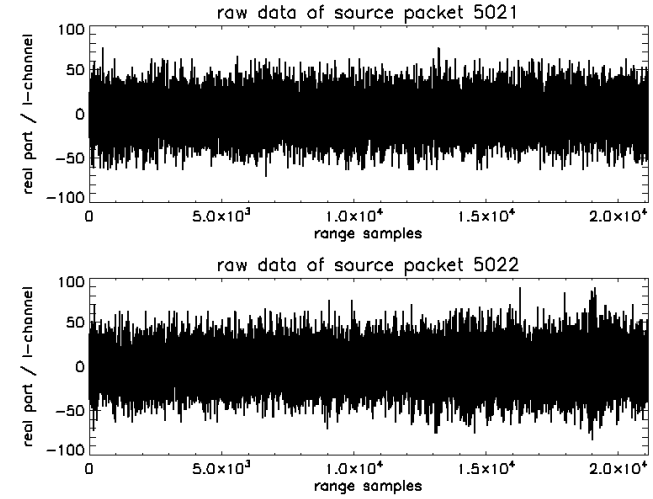

Fig. 11. Raw data of system datatake w.r.t. Fig. 2: ABOVE: rangeline containing only noise. BELOW: rangeline containing Noise and Nadir return. (only I-channel shown)

V. Margins for Digital Elevation Model

As already explained in section II.B the pre-launch approach considers only a margin at the falling edge of the Nadir return. I.e. if the PRF is selected in such way that the Nadir return rising edge happens to be directly adjacent to the focused echo window, there is no margin to compensate any other inaccuracies. Indeed, this was the case for the datatakes under investigation. The main source of error has been identified to be the inaccuracy of the Digital Elevation Model (DEM) available in the command generation. The height error map of this DEM is shown in Fig. 12.

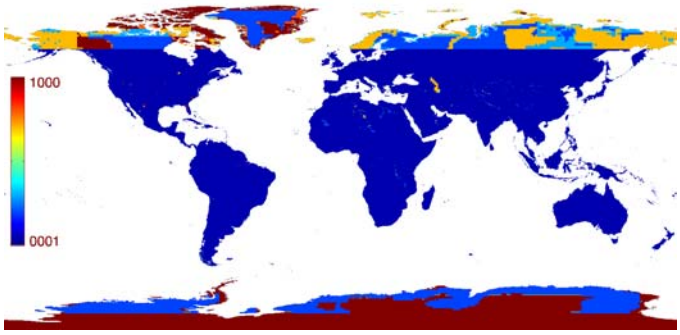

Fig. 12. Height-Error-Matrix (HEM) shows the error of the available DEM, [dark red: error = 1000 m, dark blue: error = 50 m, white: error = 1 m]

The largest error of 1000 m occurs only at the polar regions and corresponds to approximately 7 µs margin in timing. This is too large to be inserted into the timing commanding before and after the Nadir return duration, since either the PRF selection becomes impossible or the swath width is degraded. However, since the errors of 1000 m and most of the errors between 700 and 800 m occur in areas below -60° and above +60° of latitude the statistic of DEM errors in Table 1 was used to define an appropriate margin. It shows four levels of DEM errors and the corresponding global percentage of occurrence of these errors. It was found appropriate to consider DEM errors up to 300 m, which is sufficient for latitudes in between +/-60°. Outside this range of latitudes there are small swath width degradations possible in case of large DEM errors.

The conclusion was an additional margin of 2 µs before and after the Nadir return to be introduced, to consider DEM errors. After the modification of the Nadir return duration to 1.2 µs and the introduction of the DEM margins into the timing commanding, no more Nadir returns were detected.

DEM error	Timing error	percentage
50 m	**0.3 us**	**57**
(200-)300 m	**2 us**	**15**
700(-800) m	**4.7 us**	**7**
1000 m	**6.7 us**	**21**

Table 1: DEM error statistic

VI. Conclusion

The TerraSAR-X radar timing was found to be very narrow due to a small antenna and therefore the high PRF. Two pre-launch assumptions were made w.r.t. the Nadir timing, i.e. +/- 5° Nadir angle and no saturation of receiver by Nadir echoes. During the Commissioning Phase a few unwanted Nadir datatakes, i.e. 0.3 %, were identified in which visible Nadir returns appeared. These Nadir datatakes were used for analyzing and measuring the worst case Nadir width or the worst case Nadir pulse duration, respectively. The duration was determined to be 1.2 µs, which was a decrease of over 90 % w.r.t. the first assumption of around 13 µs, i.e. +/- 5° Nadir angle. After identifying mainly DEM errors as the reason for the few Nadir returns being shifted into the images, an additional DEM margin of 2 µs corresponding to 300 m DEM error was introduced before and after the Nadir return duration in the timing commanding. Nevertheless, this still led to a reduction of the overall commanded Nadir pulse width of 60 % compared to the original setting. After the update of the timing commanding no more Nadir datatakes were detected, although under extreme conditions, i.e. high DEM error at extreme geographical regions, Nadir echoes are theoretically possible. The consequence would be a small degradation in the swath width. The second assumption was confirmed, i.e. the benefit of relaxing the timing by a whole pulselength can be kept since no receiver saturation by Nadir echoes was observed.

Acknowledgment

The authors like to thank Daniel Schulze for generating the Height error matrix. Furthermore we would like to thank Marwan Younis for the very helpful discussions and suggestions.

References

[1] J. Mittermayer, R. Metzig, U. Steinbrecher, C. Gonzalez, D. Polimeni, J. Böer, M. Younis, J. Márquez Martínez, S. Wollstadt, D. Schulze, A. Meta, N. Tous-Ramon, C. Ortega Miguez: "TerraSAR-X Instrument, SAR System Performance and Command Generation", Proc. of IGARSS 2008, Boston, USA.

[2] J. Mittermayer, U. Steinbrecher, A. Meta, N. Tous-Ramon, S. Wollstadt, M. Younis, J. Marquez, D. Schulze, C. Ortega: TerraSAR-X System Performance & Command Generation, Proc. of EUSAR 2008.

[3] M. Stangl, R. Werninghaus, B. Schweizer, C. Fischer, M. Brandfass, J. Mittermayer, H. Breit: "TerraSAR-X Technologies and First Results", IEE Radar, Sonar & Navigation, 153 (2), pp. 86 – 95, 2006